Heliyon 9 (2023) e20941

Contents lists available at ScienceDirect

Heliyon

journal homepage: www.cell.com/heliyon

Synthesis, In silico mapping for anti-cancer proviso, hardness studies of D-gluconic acid monohydrate crystals for usage in electronic, mechanical and biological sectors

Padmanaban B [a], Maria P. Nikolova [b], Shashank Kumar [c], SenthilKannan K [d,*]

[a] Department of Electronics and Communication Engineering, AAA College of Engineering and Technology, Amathur, 626005, Sivakasi, Virudhunagar District, Tamilnadu, India
[b] Department of Material Science and Technology, University of Ruse "A. Kanchev", 8 Studentska Str., 7000, Ruse, Bulgaria
[c] Molecular Signaling & Drug Discovery Laboratory, Department of Biochemistry, Central University of Punjab, Bathinda, Punjab, 151 401, India
[d] Department of Physics, Saveetha School of Engineering, SIMATS, Thandalam, Chennai, 602105, TN, India

ARTICLE INFO

Keywords:
DGAMH
Mechanical
Anti-cancer
Computational
Electronic

ABSTRACT

D-Gluconic acid monohydrate - DGAMH crystals are grown in a period of 61 days by using the customary slow evaporation method with a, b and c as 8.4309, 5.409 and 10.4071 in Å units; β as 96.87°; monoclinic system, space group as $P2_1$. The material is an anticancer stipulation to inhibit them with the docked score of the DGAMH as −6.0 and −7.1 for both cases. Considering the mechanic behaviour of the DGAMH; the n as 7.57 of the DGAMH – work hardening coefficient value as Reverse ISE (indentation size effect) response for DGAMH. The computational structural info of DGAMH provides the supercell proviso, VanderWaal's impact with the nano-tubular proviso of DGAMH for cell impacting, weak type of interactions and devices with nano-tube impact. The electronic fluxing is in microns for macro-DGAMH; micro-DGAMH; thin-film DGAMH and nano-DGAMH for filtering property confirmations. The frequency by IC741 is twice over the input values with DGAMH crystal.

1. Introduction

D-Gluconic acid monohydrate – DGAMH is equilibrating properly in the case of an aqueous solution to form the mixture of lactones of γ and δ types and present case by D-Gluconic acid by direct way [1,2]. The δ one is customary available. DGAMH is one of the types of carboxylic acids which is formed by oxidizing the primary carbon of glucose which is of having profound biological and pharmacy-oriented properties.

Gluconic acid is mainly available in the plants, honey and wine. It can also be prepared by fungal fermentation methodology for commercial utility; δ-lactone structure based Gluconic acid chelating ions in the metal; specify worthy and stabilized complex-clusters and in the basic solution, this complex exhibiting strongest chelate action enroot for anions such as Cu, Fe, Al, Cl and other sorts of heavy-metallic atoms [3,4].

DGAMH is the Gluconic acid monohydrate with D configurative construction in the profile; it is a better chelating agent as mentioned above and as by the literature and is also a Penicillium metabolite. DGAMH is a conjugate of D-Gluconate and is an

* Corresponding author.
E-mail addresses: mscgoldmedalist@yahoo.in, senthilkannank.sse@saveetha.com (S. K).

https://doi.org/10.1016/j.heliyon.2023.e20941
Received 10 May 2023; Received in revised form 5 October 2023; Accepted 11 October 2023
Available online 16 October 2023

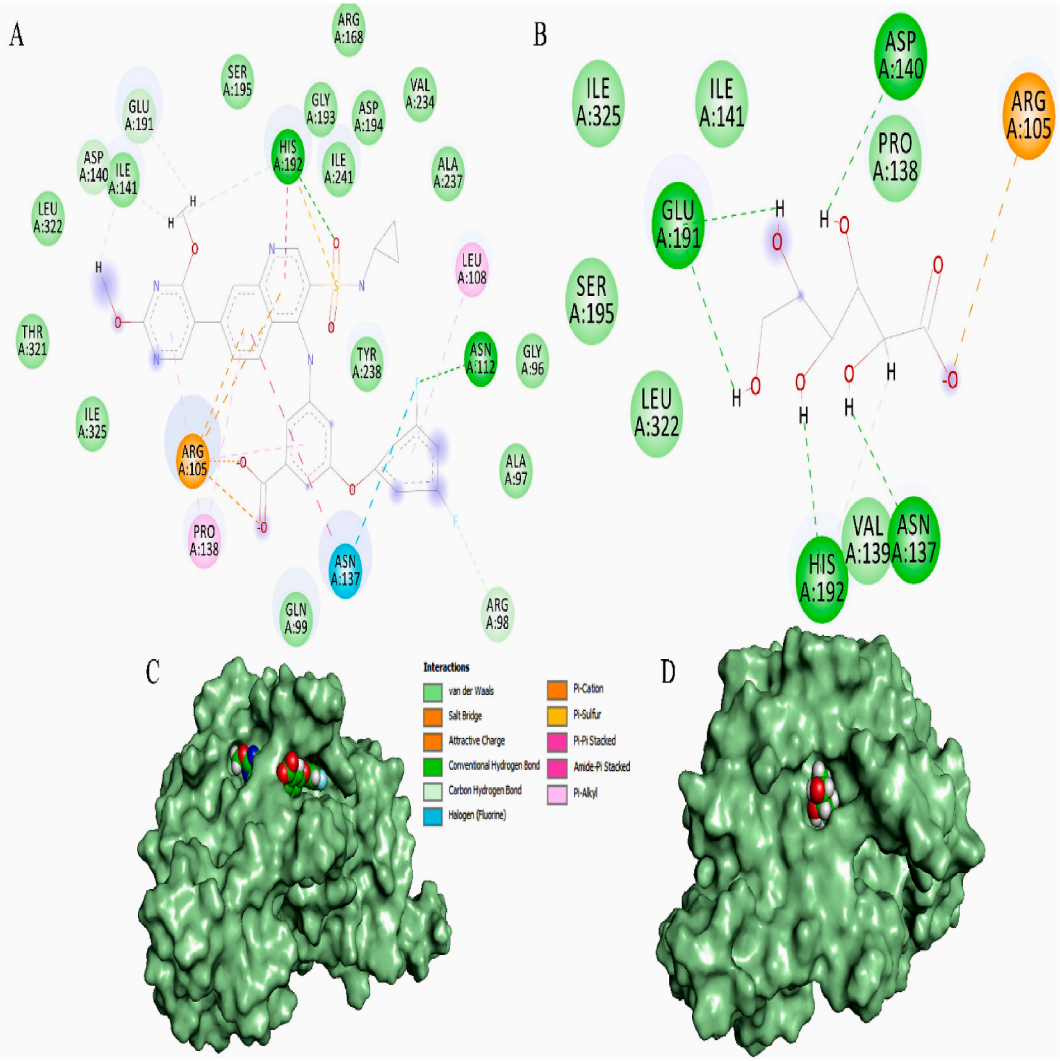

Fig. 1. Molecular docking results of lactate dehydrogenase with GSK2837808A and D-gluconic acid. (A) Interacting residues of lactate dehydrogenase with GSK2837808A. **(B)** Interacting residues of lactate dehydrogenase with D-gluconic acid. **(C)** Binding pose of GSK2837808A with lactate dehydrogenase. **(D)** Binding pose of GSK2837808A with lactate dehydrogenase.

enantiomeric tool of L-Gluconic acid. Enantiomeric relates to the pairing of molecular representations that are existing in two outlines and are of the mirror imaging portfolio of one another but are not superimposing nature to each other and simply matching by the way of chemically [5–9].

The scope of the present study is mainly to grow properly the DGAMH crystals. In general, it is a hardened process to make good-quality DGAMH crystalline specimens. It is premeditated for single crystal XRD study; molecular docking proviso; electric pulse properties; electronic studies; hardness profile; super lattice structure; Vander Waal's impacts; Supercell – Miller indices impact; nano-tubular generation of device constructing study [10–19].

2. Materials and methods

2.1. Crystal synthesis

D-Gluconic acid monohydrate crystals are obtained from D-Gluconoic acid purchased from Sigma Aldrich with water as a solvent in the customary slow evaporation methodology as this mechanism is a slow process and is very hard to proceed to be successful and tried four times to grow DGAMH crystals in 61 days. As already stated the process is difficult to grow, care is taken without shaking the system and needle-like crystals are properly grown.

Table 1
Amino acid residue interaction of lactate dehydrogenase, hexokinase with compounds for anti-cancer stipulation.

Lactate dehydrogenase			
Compound	Dock score	Hydrogen bond interaction	Hydrophobic interaction
GSK2837808A	−4.5	His192, Asn112	Gly96, Ala97, Arg98, Leu108, Ala237, Val234, Asp194, Ile241, Gly193, Arg168, Ser195, Glu191, Ile141, Asp140, Leu322, Thr321, Ile325, Arg105, Pro138, Gln99, Asn137
DGAMH	−6.0	Asn137, Asp140, Glu191, His192	Arg105, Pro138, Val139, Ile141, Ser195, Leu322
Hexokinase			
3-bromopyruvic acid	−3.2	Cys158, Asn258	Leu64, Gln160, Val207, Val206, Asn208, Phe154, Phe156, Pro157, Glu260
DGAMH	−7.1	Cys158, Phe154, Ser155, Asn208, Glu260	Leu64, Phe156, Pro157, Gln160, Val206

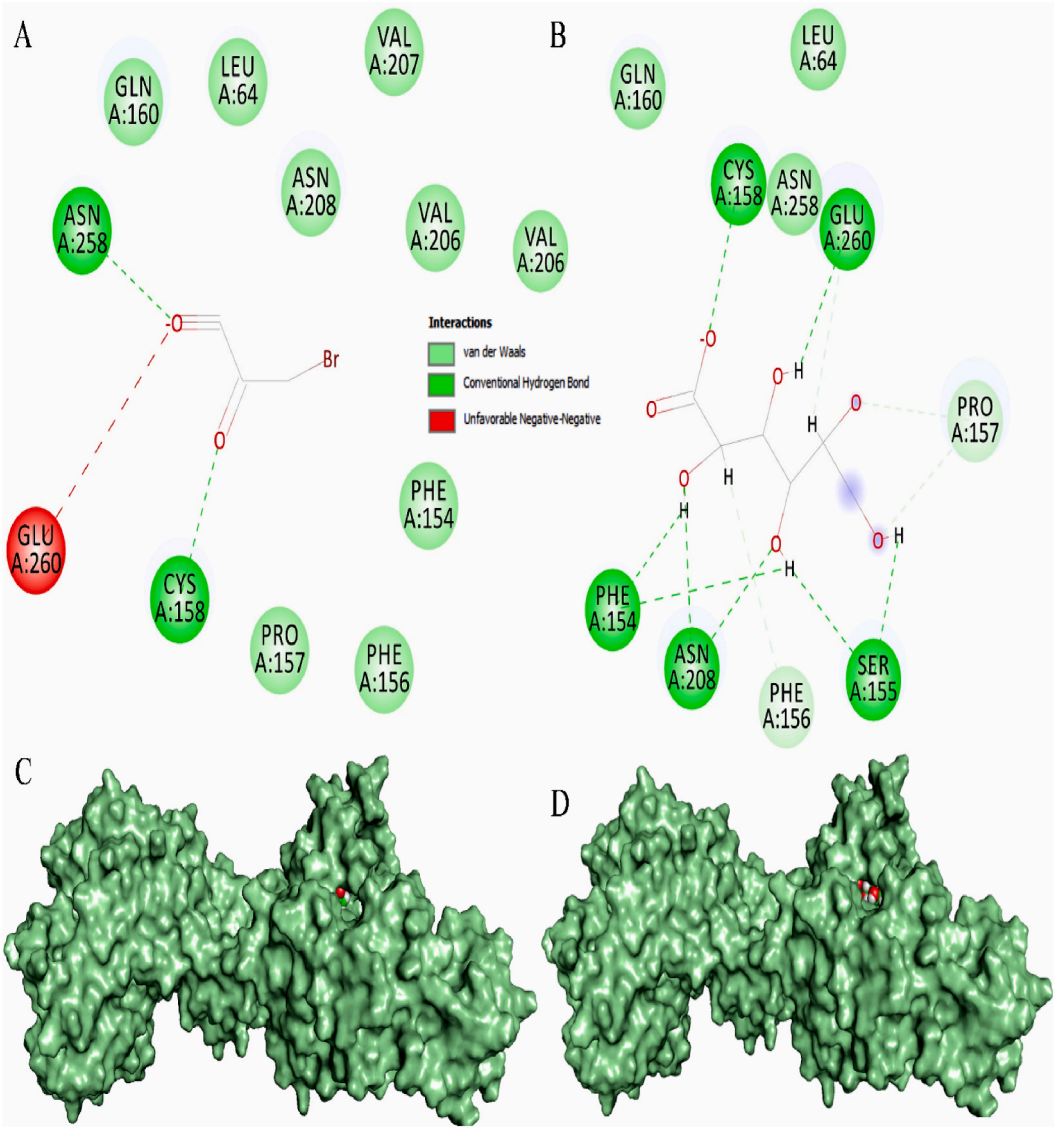

Fig. 2. Molecular docking results of hexokinase with GSK2837808A and D-gluconic acid. (A) Interacting residues of hexokinase with3-bromopyruvic acid. **(B)** Interacting residues of hexokinase with D-gluconic acid. **(C)** Binding pose of 3-bromopyruvic acid with hexokinase. **(D)** Binding pose of GSK2837808A with hexokinase.

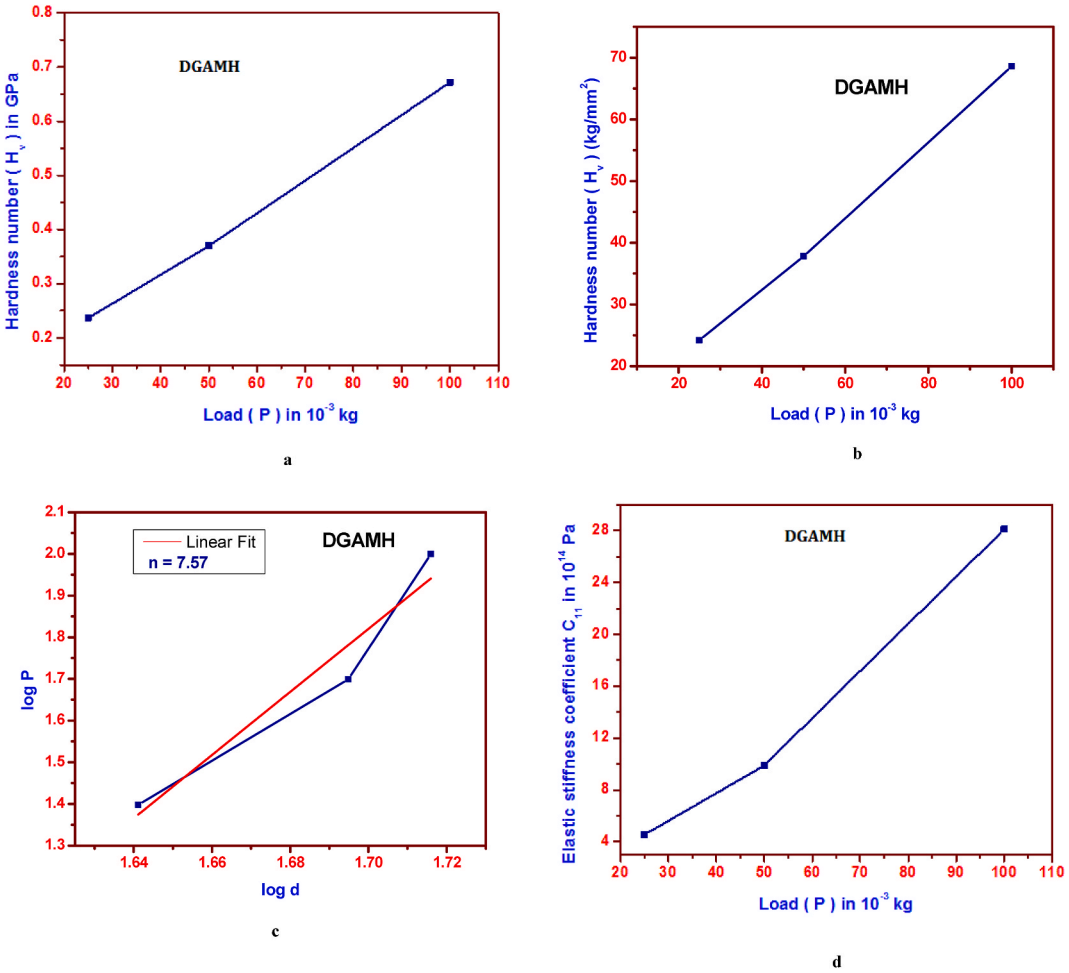

Fig. 3. a Hardness number H_V in GPa Vs load P in 10^{-3} kg of DGAMH, b Hardness number HV in kg/mm2 Vs load P in 10-3 kg of DGAMH, c Curve fitting graph for log P vs log d of DGAMH, d Elastic stiffness C11 in 1014 Pa Vs load P in 10-3 kg of DGAMH, e Young's modulus in GPa vs load P in 10-3 kg of DGAMH, f Yield strength in GPa vs load P in 10-3 kg of DGAMH, g Hardness in Mohs scale in Pa vs load P in 10-3 kg of DGAMH.

2.2. Characterization

DGAMH crystals are analyzed by Bruker Kappa Apex II XRD diffractometer. The mechanical performance is generally analyzed by the industrial utility by Vickers hardness tester, HMV-2T, Shimadzu universal testing machine) and the material's worthiness utilizing its profile related to their hardness/mechano behavior. DGAMH is analyzed with a varying load of 25, 50, and 100 g with computational tools by softwares.

2.3. In silico molecular docking and computational electronic studies

Three-dimensional structures of lactate dehydrogenase and hexokinase 2 are downloaded from the protein data bank with PDB ID of 5W8I and 5HG1. The downloaded structure of protein molecules is prepared for docking by using the protein preparation wizard of the Schrodinger software package. Three-dimensional structures of ligands are downloaded from the PubChem database and prepared for docking by using the LigPrep module of the Schrodinger software package. The receptor grid generation module is used for generating the grid for molecular docking based on the bound inhibitor in both proteins. The glide module of the Schrodinger software package is used for the molecular docking of ligands on the previously generated grid. Molecular docking of D-Gluconic Acid Mono Hydrate (DGAMH) is performed to understand its binding and interaction with lactate dehydrogenase and hexokinase. GSK2837808A and 3-bromopyruvic acid are used as the known inhibitors of lactate dehydrogenase and hexokinase respectively. The Computational, electronic studies of DGAMH crystals are done with the docking software, Jmol, chemdraw software and nano-tube generating tool and by diodes.

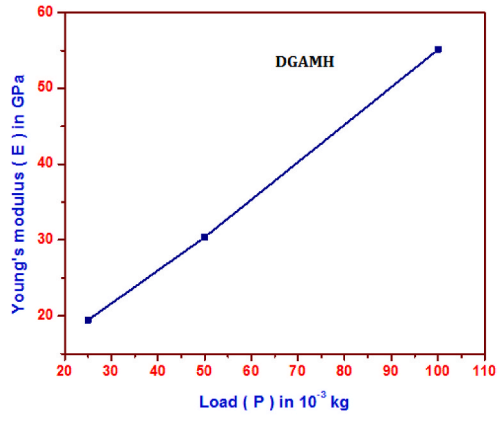

e

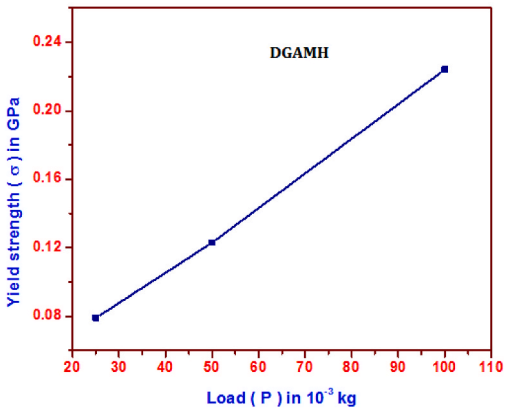

f

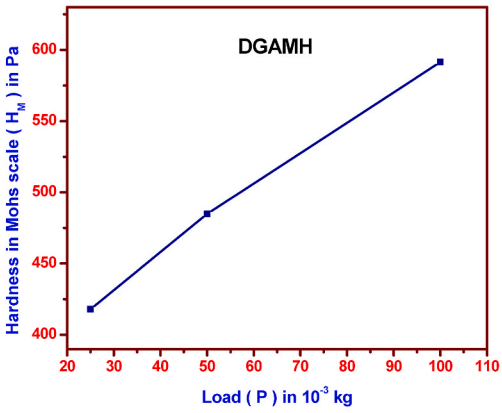

g

Fig. 3. (*continued*).

3. Results and discussions

3.1. Structure and molecular docking

3.1.1. Single crystal XRD pattern of the DGAMH crystals

The XRD data of the D-Gluconic acid monohydrate crystals are as specified below; the obtained values indicate bond lengths and bond angles as follows: a, b and c equal to 8.4309, 5.409 and 10.4071 Å, respectively; $\alpha = \gamma = 90^{\circ}$ and β as 96.87° corresponding to monoclinic system with space group as $P2_1$.

3.1.2. Docking proviso

D-gluconic acid formed four hydrogen bonds with lactate dehydrogenase in comparison to the known inhibitor GSK2837808A which formed two hydrogen bonds (Fig. 1 A-D). Hydrogen bond forming and hydrophobically interacting residues of lactate dehydrogenase with GSK2837808A and D-gluconic acid are given in Table 1. In the case of hexokinase, D-gluconic acid formed five hydrogen bonds in comparison to known inhibitor 3-bromopyruvic acid which formed two hydrogen bonds with hexokinase (Fig. 2 A-D). Hydrogen bond forming and hydrophobically interacting residues of hexokinase with 3-bromopyruvic acid and D-gluconic acid are given in Table 1.

3.2. Mechanical behaviour of DGAMH crystals

The hardness of DGAMH crystals analyzed with a load of 25, 50, and 100 g is found to be equal to H_V 24.9, 44.8, and 68.6 kg/mm^2, respectively and as 0.237, 0.370, and 0.672 in GPa, respectively, as mentioned in Fig. 3(a) and (b). The linear fitting of the log P vs log d data is provided in Fig. 3 (c); the n as 7.57 the DGAMH – work hardening coefficient value: with the increase of the load values the H_V values are also elevated while having reverse indentation size effect (ISE) response. Fig. 3(d) for elastic stiffness of DGAMH as the small

Table 2
Load vs H_v in kg/mm^2 of DGAMH crystalline sample of macro-scale.

Load P in 10^{-3} kg	Hardness (H_V) in kg/mm^2
25	24.9
50	44.8
100	68.6

Table 3
H_V in GPa, Stiffness, Young's modulus and Yield strength of DGAMH crystalline sample of macro-scale.

P in 10^{-3} kg	Hardness (H_V) in GPa	Elastic stiffness coefficient C_{11} in 10^{14} Pa	Young's modulus E in GPa	Yield strength σ in GPa
25	0.237	4.53	19.44	0.079
50	0.370	9.90	30.38	0.123
100	0.672	28.10	55.14	0.224

Table 4
Hardness in Mohs scale of DGAMH crystalline sample of macro-scale.

P in 10^{-3} kg	Hardness in Mohs scale (H_M) in Pa
25	417.89
50	484.89
100	591.46

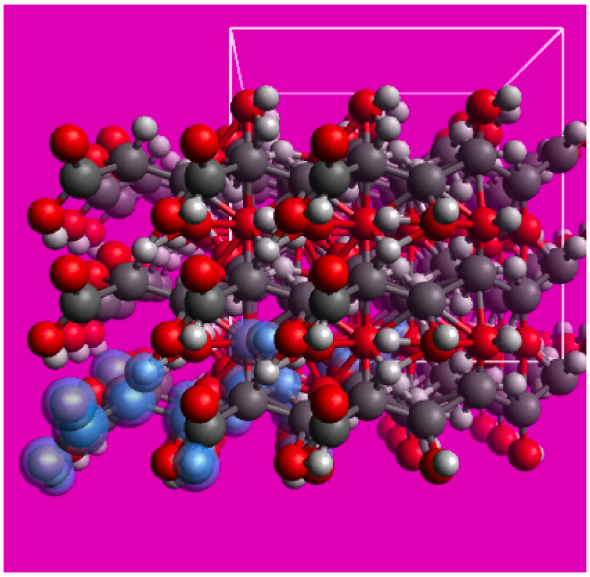

Fig. 4. 3*3*3 Supercell impact of DGAMH crystals.

bent is observed at 50 g profile and more variation is observed in the data of 100 g profile as the values are 4.53, 9.90 and 28.10 in the units of 10^{14} Pa.

The Young's modulus profile of DGAMH as in Fig. 3 (e) portrays the linear curve and the values are gradually prolonged as 19.44, 30.38 and 55.14 in GPa and similarly, Fig. 3(f) portrays the gradually prolonged Yield strength parameters as 0.079, 0.123 and 0.224 in GPa. The hardness in the Mohs scale is portrayed as in Fig. 3(g) and no variations in 25 g and 50 g are observed and small variations are experiential in 100 g profile in Mohs scale as 417.89; 484.89 and 591.46 in Pa. The corresponding data are observed and tabulated in Tables 2–4, respectively. Based on the data from Tables 2–4 and by the mechanical hardness data; the macro-DGAMH [8–10] can be pronounced for rheology or tribology proviso and here, tried for a circular wire of helix spring category as continued.

The tribological work deals with the wear along with the tear of the trial which can be applied with the circular wiring with helical springs with DGAMH macro-crystal of shiny surface effect. The single coil with a shear of 0.62 GPa, and a string stiffness of 10 N/m. The parameters represent the effectiveness with proper stress, deflective values of the entitled sample, and the impact over electronic devices and in mechano-elastic industries for the existence of coil or spiral spring for improved firmness of macro scales, which is

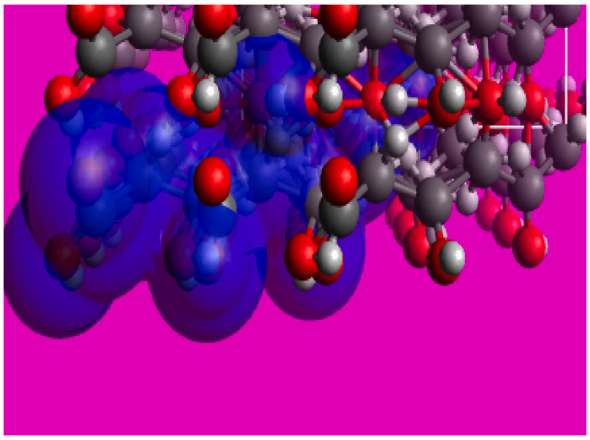

Fig. 5. VanderWaals with 3*3*3 super cell impact of DGAMH crystals.

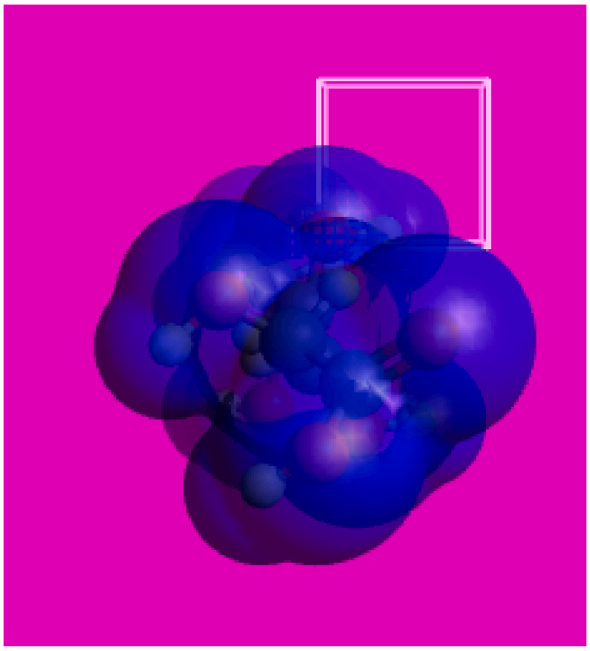

Fig. 6. VanderWaals impact on DGAMH without potential outcome.

termed as macro-tribology of DGAMH crystals [11–19].

3.3. Computational electronic studies of DGAMH crystals

The supercell proviso of 3*3*3 case of DGAMH is portrayed for special volume cell as in Fig. 4, to identify the prolonged use and extended interactions; the weak interaction stipulation of DGAMH by VanderWaal's impact is as shown in Fig. 5 for identifying the nature of the type of interactions and the weak proviso, without and with the impact of the electrostatic potential effect of Vander-Waal's is shown in Figs. 6 and 7. The supercell proviso of 3*3*3 case with 3*3*3 of Miller's impact is shown in Fig. 8; with the nano-tubular proviso of DGAMH is presented in Fig. 9.

The electronic versatile functionality of DGAMH as a functional material for frequency doublers and as an influx generator is 2.9979, 3.4373, 3.9998 and 4.0309 μm for macro-DGAMH; micro-DGAMH; thin-film DGAMH and nano-DGAMH for filtering property by in fluxing values. The frequency doublers as in the case of an op-amp by IC741 is twice over the input values and for macro-DGAMH; micro-DGAMH and nano-DGAMH as 2.070; 2.05; 2.02 times the input values for recurrence relations as in Fig. 10 for influxing proviso [18–20].

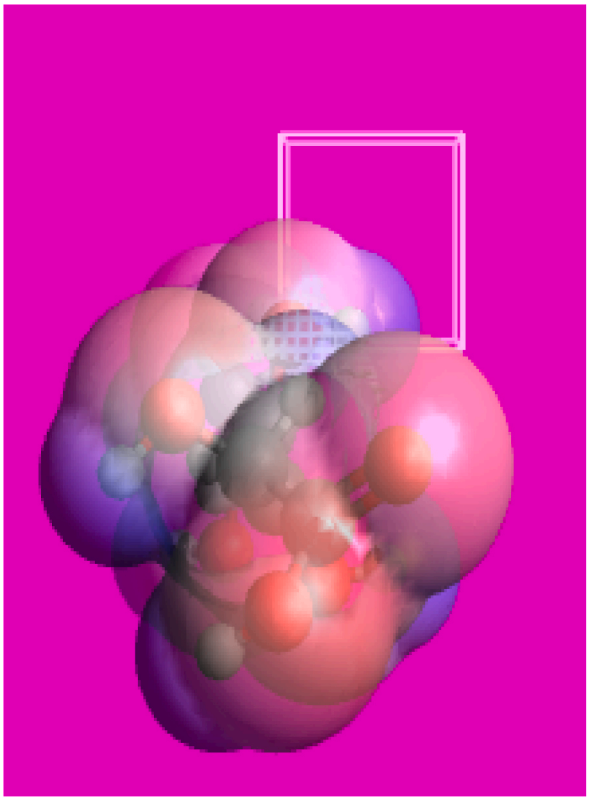

Fig. 7. VanderWaals impact on DGAMH with the coloured potential upshot.

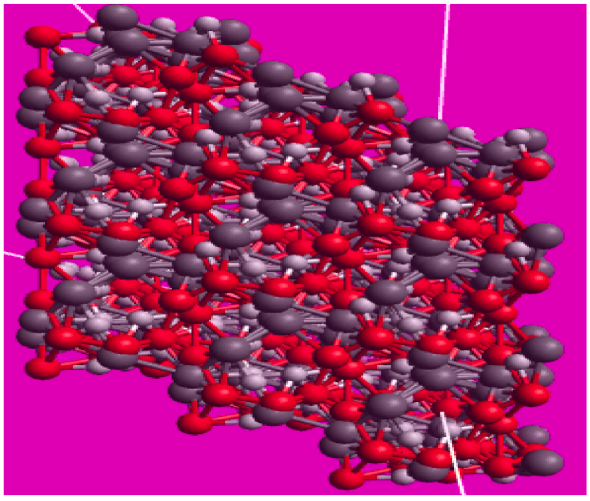

Fig. 8. 3*3*3 Super cell builder in 3*3*3 Miller indices of DGAMH.

4. Conclusion

D-Gluconic acid monohydrate - DGAMH crystals are appropriately grown in 61 days by using the traditional slow evaporating process using water as solvent. Their crystal structure belongs to a monoclinic system with a space group $P2_1$. The material is identified to be the better scope for anti-cancer specification to inhibit dehydrogenase and hexokinase by docking. Taking into the consideration of the mechanical behaviour of the DGAMH, it is shown that the n is 7.57 of the DGAMH while the work hardening coefficient value demonstrated reverse indentation size effect (ISE) response. The computational structural info of DGAMH provides the supercell proviso of 3*3*3 case with VanderWaal's and Miller's impact with the nano-tubular proviso of DGAMH for use in devices and in

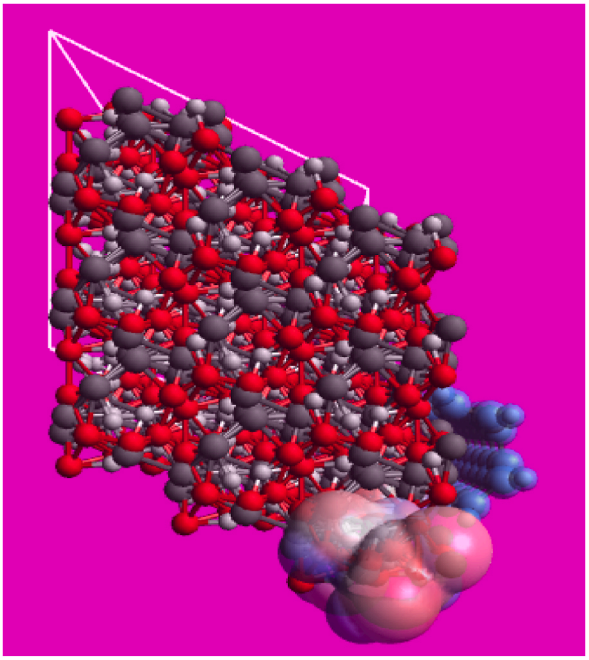

Fig. 9. 3*3*3 Supercell with 3*3 of n, m and of tube length as 22 nm of DGAMH with weak interactions.

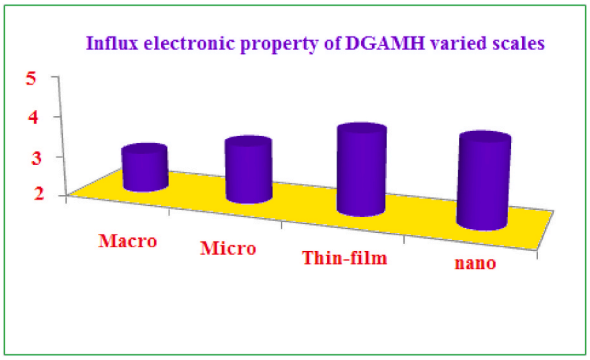

Fig. 10. Influx data for the electronic property of DGAMH at different scales.

gadgets. The electronic influxing is equal to 2.9979, 3.4373, 3.9998 and 4.0309 μm for macro-DGAMH; micro-DGAMH; thin-film DGAMH and nano-DGAMH, respectively, for filtering properties and frequency enhancement.

Funding

This publication is developed with the support of Project BG05M2OP001-1.001-0004 UNITe, funded by the Operational Programme "Science and Education for Smart Growth", co-funded by the European Union trough the European Structural and Investment Funds.

Ethics statement

The paper is reported as new work and not reported anywhere as partly or simultaneously. New work consigning anti-cancer by docking and all type of mechano representation.

Data availability statement

No data was used for the research described in the article. All inferences are reported.

CRediT authorship contribution statement

Padmanaban B: Formal analysis, Investigation. **Maria P. Nikolova:** Data curation, Formal analysis, Funding acquisition. **Shashank Kumar:** Formal analysis, Investigation, Methodology. **SenthilKannan K:** Conceptualization, Data curation, Formal analysis, Investigation, Methodology, Project administration, Resources, Software, Supervision, Validation, Visualization, Writing – original draft, Writing – review & editing.

Declaration of competing interest

The authors declare that they have no known competing financial interests or personal relationships that could have appeared to influence the work reported in this paper.

References

[1] W.C. Oliver, G.M. Pharr, Measurement of hardness and elastic modulus by instrumented indentation: advances in understanding and refinement of methodology, J. Mater. Res. 19 (2004) 3–20.
[2] L. Pizzagalli, Stability and mobility of screw dislocations in 4H, 2H, and 3C, silicon carbide, Acta Mater. 78 (2014) 236–244.
[3] T. Csanádi, M. Bl'anda, N.Q. Chinh, P. Hvizdoš, J. Dusza, Orientation-dependent hardness and nanoindentation-induced deformation mechanisms of WC crystals, Acta Mater. 83 (2015) 397–407.
[4] W.G. Mao, J.M. Luo, C.Y. Dai, Y.G. Shen, Effect of heat treatment on deformation and mechanical properties of 8 mol% yttria-stabilized zirconia by Berkovich nanoindentation, Appl. Surf. Sci. 338 (2015) 92–98.
[5] L. Chen, A. Ahadi, J. Zhou, J.E. Ståhl, Modeling effect of surface roughness on nanoindentation tests, Procedia CIRP 8 (2013) 334–339.
[6] W.D. Nix, H. Gao, Indentation size effects in crystalline materials: a law for strain gradient plasticity, J. Mech. Phys. Solid. 46 (1998) 411–425.
[7] Y.S. Chou, D.J. Green, Silicon carbide platelet/alumina composites: II, mechanical properties, J. Am. Ceram. Soc. 76 (1993) 1452–1458.
[8] A. Dey, A.K. Mukhopadhyay, S. Gangadharan, M.K. Sinha, D. Basu, N.R. Bandyopadhyay, Nanoindentation study of micro plasma sprayed hydroxyapatite coating, Ceram. Inter. 35 (2009) 2295–2304.
[9] A.C. Fischer-Cripps, Introduction to Contact Mechanics, second ed., Springer, NewYork, 2007.
[10] S. Goel, J. Yan, X. Luo, A. Agrawal, Incipient plasticity in 4H-SiC during quasistatic nanoindentation, J. Mech. Behav. Biomed. Mater. 34 (2014) 330–337.
[11] S. Goel, The current understanding on the diamond machining of silicon carbide, J. Phys. D Appl. Phys. 47 (2014) 1–36.
[12] I. Inasaki, Grinding of hard and brittle material, CIRP Ann. Manuf. Technol. 36 (1987) 463–471.
[13] K.L. Johnson, The correlation of indentation experiments, J. Mech. Phys. Solid. 18 (1970) 115–126.
[14] J.H. Lee, Y.F. Gao, G.M. Pharr, Effective Poisson's ratio from combined normal and lateral contacts of single crystals, J. Mater. Res. 27 (2012) 182–191.
[15] X. Li, X. Wang, R. Bondokov, J. Morris, Y.H. An, T.S. Sudarshan, Micro/nanoscale mechanical and tribological characterization of SiC for orthopedic applications, J. Biomed. Mater. Res. Part B: Appl. Biomater. 72B (2005) 353–361.
[16] W.G. Mao, Y.G. Shen, C. Lu, Deformation behavior mechanical properties of polycrystalline and single crystal alumina during nanoindentation, Scr.Mater. 65 (2011) 127–130.
[17] K. Suganya, J. Maalmarugan, R. Manikandan, et al., J. Mater. Sci. Mater. Electron. 33 (2022), 19320, https://doi.org/10.1007/s10854-022-08770-0.
[18] V. Sathiya, K. Suganya, K. SenthilKannan, et al., J. Mater. Sci. Mater. Electron. 33 (2022), 19514, https://doi.org/10.1007/s10854-022-08787-5.
[19] X. Vasanth Winston, D. Sankar, K. SenthilKannan, et al., J. Mater. Sci. Mater. Electron. (2022), https://doi.org/10.1007/s10854-022-08873-8.